Dosimetry and Microdosimetry using COTS ICs: A Comparative Study

Leif Scheick, Gary Swift, Steve Guertin, David Roth, Peter McNulty, and Duc Nguyen

ABSTRACT

A new method using an array of MOS transistors for measuring dose absorbed from ionizing radiation is compared to previous dosimetric methods. The accuracy and precision of dosimetry based on COTS SRAMs, DRAMs, and UVPROMs are compared and contrasted. Applications of these devices in various space missions will be discussed. TID results are presented for this summary and microdosimetric results will be added to the full paper. Finally, an analysis of the optimal condition for a digital dosimeter will be presented.

INTRODUCTION

Electron-hole pairs are generated in all areas of the circuit when ionizing radiation interacts with microelectronic circuits. Some of these electrons and holes are bound in the various oxides of the structures that make up the integrated circuit. One of the most susceptible single unit electronic items is the MOSFET, or more specifically the oxide between the gate and the channel is very sensitive to radiation effects. In fact, the RADFET dosimeter is based on a MOSFET specifically designed to increase threshold change of the transistor as a function of radiation. The RADFET has several liabilities in measuring dose directly, but the most prevalent is that the support electronics needed to maintain the correct currents and voltage to measure to threshold change are prohibitive to most remote measurement needs.

THEORY

The three types of memories surveyed here all are based on voltage shift is the MOS capacitor. The UVPROM also measure the bias shift due to the removal of electrons from the floating gate. In this section, the basic mechanisms from which the absorbed dose can be measured are described. The full paper will explore the device physics in more depth. Table 1 describes the basic elements of each method.

The memory cell of a CMOS SRAM contains 6 MOSFETS. Typically, two p-channel and four n-channel devices make up the SRAM cell. Each of these should respond to radiation like regular MOSFETs. SRAMs have been studied extensively for TID and SEE response [1]. Now unlike discrete MOSFETs, the MOSFETs that make up a SRAM cell may not have a think oxide so the positive bulk trapping should be negligible. The interface threshold shifts should be the main radiation effect. This will tend to keep the actually SRAM inverter fairly robust in terms of holding the memory state after irradiation. The access transistors should demonstrate the largest radiation induced threshold shift. The technique to use a SRAM as a dosimeter is to program the device as one would normally. The bias on the SRAM is ramped down and read at reduced bias on the Vcc and all input pins. At some voltage, the number of cells that cannot maintain the programmed state should change with dose.

The theory of UVPROM based floating gate dosimetry has been well documented in previous studies [2]. For this study, the fundamental idea is the same. The charge removed from the floating gate by radiation can be measured since the charge is a monotonically decreasing amount with dose. This method uses short duration programming pulses on the device as the metric of measuring dose. Sufficiently small programming pulses should be able incrementally load the floating gate with electrons. Pulse length can range from nanoseconds to milliseconds and both the Vpp and Vcc can be varied to minimize noise or increase response. All other aspects of this study will parallel previous UVPROM dosimeter investigations to discern the change in accuracy and precision of the method of using change in erasure time with UV as the metric of dose measurement.

A DRAM cell consists of a capacitor and a transistor. The capacitor stores the bit of information and the transistor isolates the capacitor during non-read or non-write times, which is approximately 99% of the time. During this time, the cell experiences subthreshold leakage that causes the DRAM cell to lose its programmed state. Thus, the cell needs to be refreshed, i.e., rewritten, occasionally. If it is not refreshed, the cell will eventually fail to retain its datum. This time to fail should decrease as a function of radiation exposure, and this effect is the foundation of the paper. Measuring the retention time for a DRAM is complicated, since the DRAM automatically refreshes the cells after a read. The manufacturer specifies a refresh time of 64ms, which is the maximum time between rewrites that data is guaranteed to remain in the cells without error. Measurement of the retention time of a cell is determined by writing to the DRAM and not accessing the device for the desired amount of time. The device is then readout, and the bits that report an error are recorded. This cycle is then repeated for another desired measurement of the retention time until a curve of bit errors versus time of desired precision is acquired. See [3] for fuller description.

Table 1

Device	Technology	Metric	Units
SRAM	CMOS	Voltage Shift	Volts
DRAM	CMOS	Retention Time	Seconds
UVPROM	FAMOS/CMOS	Programming Cycles	Cycles

PROCEDURE AND SETUP

The devices used in this study were WMS128k8 SRAMs in a 128kx8 bit format, Toshiba TC51648065APT DRAMs,

the AM27C64 CMOS FAMOS FET UVPROM in an 8192x8 bit format.

The test equipment was comprised of two PCs, a power supply, and a specially designed test board. One PC controlled a HP6629A power supply. A dedicated PC controlled the test circuit board designed specifically for this SRAM test to read and write to the DUTs. This setup allows complete freedom to interact with the DUT. See [1-3] for respective description of each experimental setup.

RESULTS

A. DRAM results

Since most of the distribution is due to variance across the device, and not retention time variance, permanent changes in the retention time distribution are due to radiation effects. These results will be very valuable when considering the single cell effects below. These results also show that cells have different susceptibility to damage.

The change in the cumulative number of errors for various gamma exposures is shown in Figure 1. Figure 1 also shows fits for each data set. The radiation source was gamma from the JPL Colbalt-60 room irradiator. The data are fit by the empirical function:

$$N = N_0\left(1 - e^{-\left(\frac{t}{t_0}\right)^\alpha}\right)^\beta , \qquad (1)$$

where t_0, α, and β are constants. N is the number of errors at time t, and N_0 is the total number of DRAM cells.
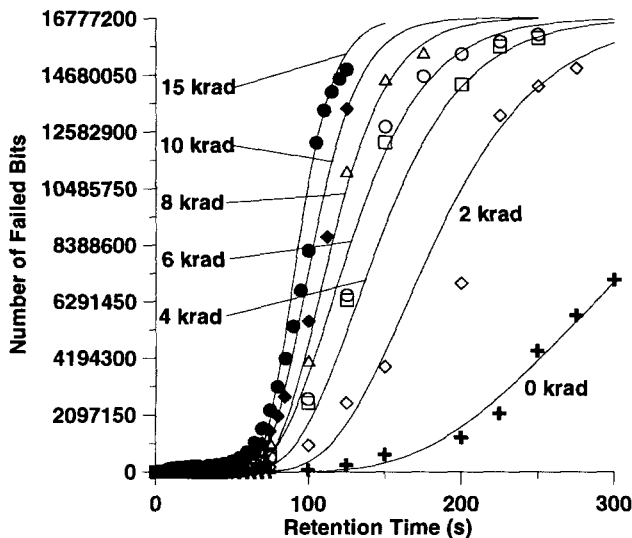

Figure 1. Retention time of a Toshiba 16 Mb DRAM due to different radiation exposures. The change in the structure of the curves indicates a total dose effect.

Figure 2 demonstrates a very useful result. Plotted is the normalized retention time needed for one half of the DRAM cells to report an error. This allows a method of equating retention time shift with an average dose per DRAM cell. Figure 2 is derived by fitting (1) to the data in Figure 1 and

then solving for t, where $N = N_0/2$. The dose that a DRAM cell has received can be determined by using Figure 3 as a calibration.
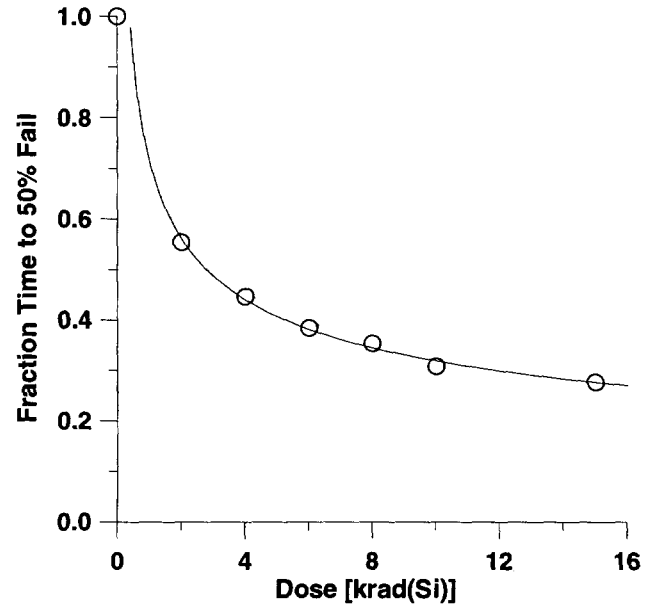

Figure 2. The retention time required to record 50% errors on the device as a function of dose. This is, in effect, the median change in retention time, which can be used to estimate the dose absorbed by a single DRAM cell. The data obeys a power law fit with an exponent of -0.35.
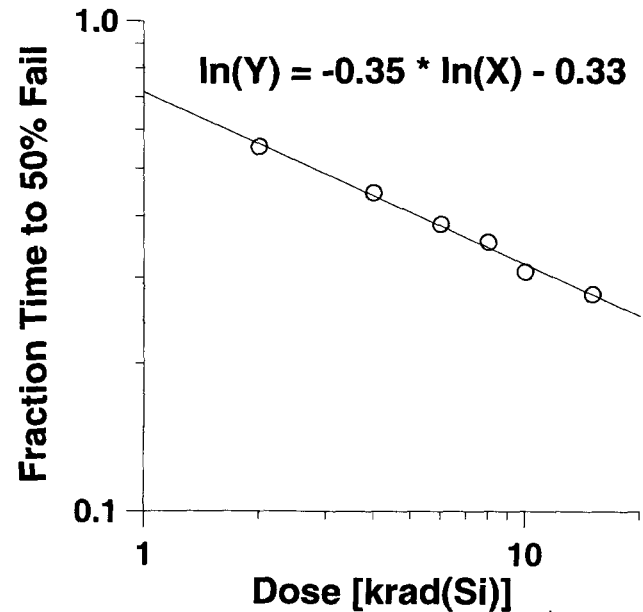

Figure 3. The retention time required to record 50% errors on the device as a function of dose. This is, in effect, the median change in retention time, which can be used to estimate the dose absorbed by a single DRAM cell. The data obeys a power law fit with an exponent of -0.35.

The most probable application of the DRAM as a dosimeter is for a circuit involving a monostable multivibrator can incremental delay the refresh time to measure how long the device takes to have 50% fail. The delay can be latch into a flip-flop and therefore read into a computer. The full paper will explore this application.

B. SRAM results

The result of a device being irradiated to 30krad in 10krad steps is shown in Figure 4. The shift is toward higher voltages at which the device can no longer hold its state. If the device is readout below this bias, and then readout above the threshold bias, the correct pattern is recovered. This shows that for this protocol, the access transistor is experiencing the threshold shift. If the pins are not allowed to float during irradiation, this behavior may change. The application here would be to load a pattern into a SRAM designated for TID measurement and sweep through voltages when a measurement is desired. The change in operating bias that yields the 50% duty cycle would correlate to dose.
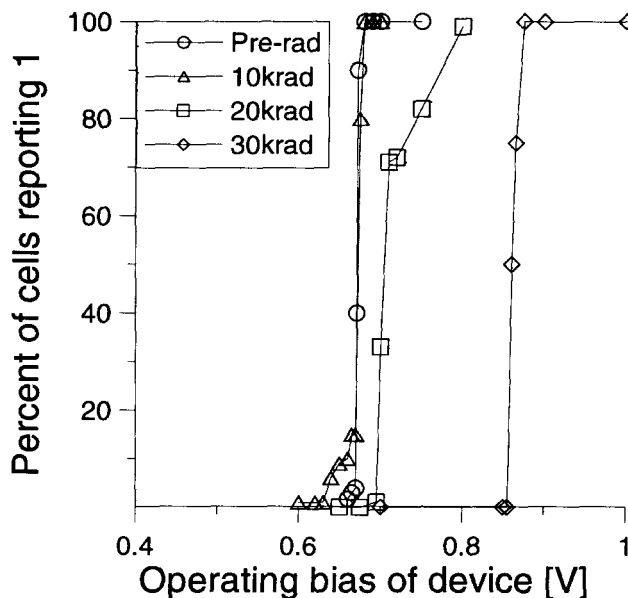

Figure 4   The percent of memory states to flip (0 to 1) as a function of the readout bias for four different TID levels.

A calibration curve for this protocol is shown in Figure 5. The change is small when compared to digital levels but easily programmable with digital to analog converter. A process could easily control voltage and measure the number of cells not reporting as programmed.

A more elucidating analysis is shown in Figure 6. The change in biasing at which 50% of the cells fail to report the state to which each was programmed is plotted versus TID level on a log-log scale. It is clear that change in bias is the metric and depends on applied dose in a power law relationship. The ramifications of this effect and its cause will be investigated in the full paper.

The most probable application of the SRAM as a dosimeter is for a circuit dropping bias, from discharging capacitor for example, and the bias to which 50% of the cells fail correlated with dose. This bias is linear with the number of reads the system must perform. The full paper will explore this application.

C. UVPROM Results

Since UV light removes electrons from the floating gate, being able to measure the DUT response to UV is an

important benchmark. Figure 7 shows the response of DUT used to measure UV. A completely erased curve as well a several levels of exposure to UV are included. These are typical curves, and the non-smooth levels are typical of DUT noise. Figure 8 shows the amount of programming time required to return the device to a programmed state. The relation is linear, as expected. The error bars reflect root-N deviation due to the low amount of readings the systems can report on low UV exposures. Figure 7 and Figure 8 illustrate the method of using the device as a general dosimeter.
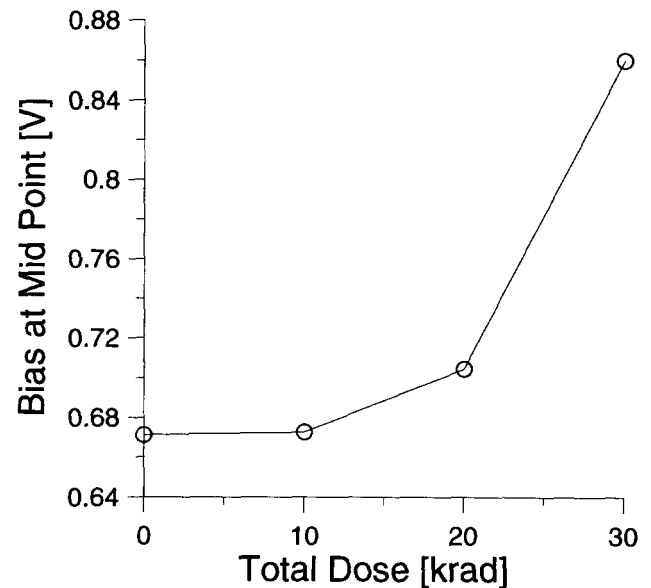

Figure 5   The readout bias at which 50 percent of the cells could not report the 1 that each was programmed. The ordinate values are found by calculating at what bias there is 50% response from the traces in Figure 4.
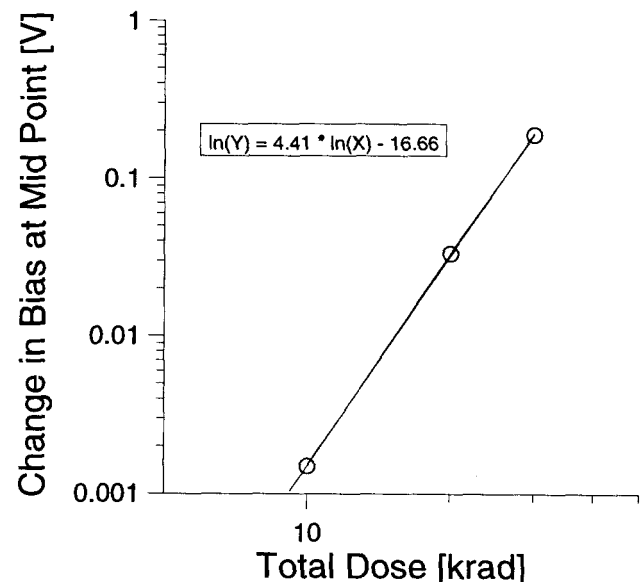

$$\ln(Y) = 4.41 * \ln(X) - 16.66$$

Figure 6   The change in readout bias at which 50 percent of the cells could not report the 1 that each was programmed. The ordinate values are found from Figure 5 by subtracting the bias value at each level by the bias at 0 krad.

Number of Programmed Bits vs. Programming for Various Programming Pin Volatges
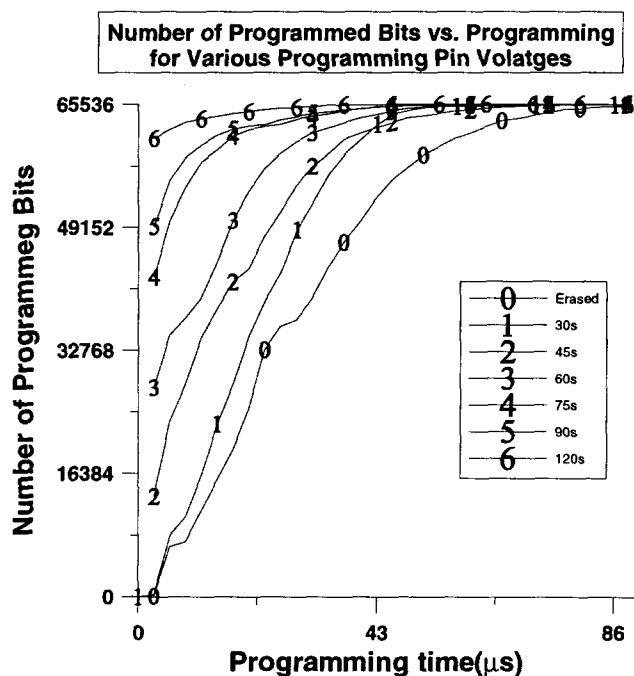

Figure 7. A total dose measurement run using UV as the radiation. This is a typical curve that shows the DUTs sensitivity to noise. Averaging compensates for the noise issues.
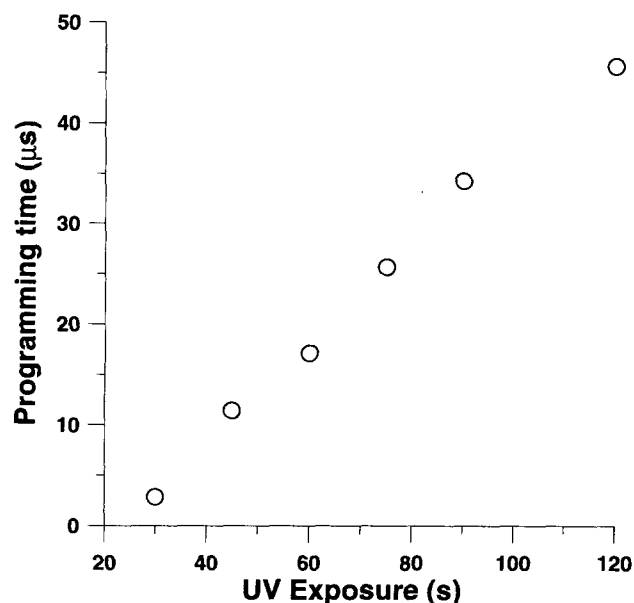

Figure 8. A total dose measurement run using UV. This relationship was expected to be linear and is seen to be. Since the UV does not damage the device or limit endurance lifetime, this relationship reveals the upper bound of the system's precision.

Measurement of gamma from the JPL Cobalt-60 source at 50 krad(Si)/s is shown in Figure 9. Results from two DUTs are shown. The response is non-linear and has a power law response. The exponent of the power law is approximately 0.8. Gamma was expected to exhibit a similar response to measurements done in previous studies with this device.

An important note concerning irradiation should be illustrated here. The response of the FAMOS cells to short pulse programming changes for an irradiated device. The voltage on the Vpp pin should be increased after irradiation.

A Vpp of 9.2V to 9.5V is used for irradiated devices. This change in Vpp is due to charge building up in the channel oxide due to irradiation and has not been seen to anneal. The response of the dosimeter remains intact.

The most probable application of the UVPROM as a dosimeter is for a circuit involving a DAC to bias the Vpp pin of the device then count the number of pulse require to return each bit to the programmed state. The full paper will explore this application.
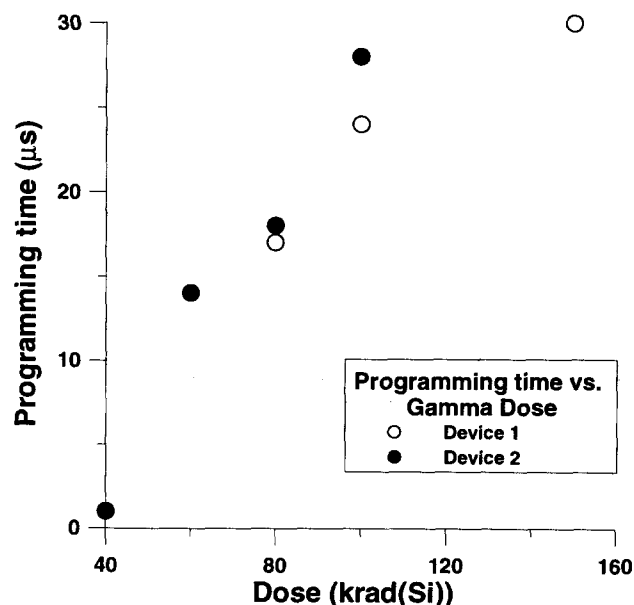

Figure 9: Total dose repsonse of two different devices of two different ion at BNL. The relationship is a power law and aggrees with earlier studies.

Table 2.

Device	Precision	Dynamic Range	Speed Rank
SRAM	~10 Rad	30 krad	1
DRAM	~100 Rad	20 krad	2
UVPROM	~10 Rad	100 krad	3

CONCLUSIONS

The full version of this paper will detail the microdosimtery applications of these devices as well as explore the dosimetric potential of hybrid devices and other technologies like FPGAs and novel non-volatile memories. Table 2 shows a comparison of the methods. Also, results from the MPTB application of the UVPROM dosimeter will be reviewed.

REFERENCEs

[1] Scheick, L and G. Swift. "Dose Measurement based on Threshold Shift in MOSFET arrays in Commercial SRAMS", Nuclear Science, IEEE Transactions on , To be publsihed Dec. 2002

[2] Scheick, L, S. Guertin and G. Swift. "Analysis of Radiation Effects on Individual DRAM Cells", Nuclear Science, IEEE Transactions on , Volume: 46 Issue: 6 Part: 1 , Dec. 1999 Page(s): 1342 -1353

[3] Scheick L., P. McNulty, D. Roth, and L. Dusseau , "UVPROM Dosimetry Aboard The MPTB Satellite: Method Optimization And Implementation" RADECS , , Dec. 2001.